2023 European Control Conference (ECC)
June 13-16, 2023. Bucharest, Romania

Optimal Target Capture and Station Keeping Control of Mobile Agents without Global Position Information

Ahmed Fahim Mostafa[1], Barış Fidan[1], and Samet Güler[2]

Abstract— **The target capture problem, i.e., the problem of reaching a target zone, by a mobile robotic agent that cannot sense its own global position requires reactive motion control algorithms based on onboard sensor data. Although the existing solutions to the target capture problem provide robust convergence guarantees, they do not address the mobile agent's path and motion optimality. We address the agent path and motion optimality in target capture control and its extension to station keeping, i.e., steering the agent to a location that is pre-defined with respect to a set of beacons, in global positioning system (GPS)-denied environments. We formulate optimal control problems aiming to minimize the agent-target distance for target capture, and the difference of desired and actual agent-station distances for station keeping. We design and analyze a linear quadratic optimal control scheme involving a Luenberger observer based state estimator, for each of the target capture and station keeping problems. The proposed schemes outperform the previous approaches in numerical simulations in terms of agent path length and smoothness.**

I. INTRODUCTION

Conventional mobile robot path planning methods navigate a robot (or vehicle) agent from a start pose (location and orientation) to a target pose through an optimal, collision-free path within the workspace [1]. If the target pose is unknown or a global positioning system (GPS) is unavailable, then the conventional methods cannot be applied directly, and the agent can utilize only the relative (e.g., distance and bearing) measurements through its onboard sensors to reach the target. For instance, in [2], a group of unmanned aerial vehicles (UAVs) search for an unknown target location in a search-and-rescue application utilizing the received signal strength (RSS) of radio frequency (RF) signals from the target. In [3], UAVs aim at localizing marine targets exploiting the angle-of-arrival (AOA) of the signals transmitted by these targets.

The problem of navigating mobile robotic agents via relative measurements in GPS-denied environments have been investigated in a list of works [4]–[12]. The problem is approached in [4] as a source seeking objective and an extremum seeking controller is designed to drive a unicycle vehicle to a target from which the vehicle receives signals in the form of a function of distance. For convergence, a persistently exciting signal is added to the angular velocity, which causes orbit-like trajectories.

Since the variable of interest for *target capture*, i.e. reaching a target zone, and circumnavigation around the target is the robot-target distance, several works have exploited polar coordinate representations in the control design [5], [6], [8], [10]. A switching-based control law for nonholonomic vehicles is proposed in [5] to circumnavigate a UAV around a target utilizing the UAV-target range and range-rate measurements. In [6], [7], range-rate estimation is integrated to circumnavigation control. The works [8], [10] propose switching-based control laws together with range-rate estimation methods for the target capture objective. Although the experimental results of [10] on a nonholonomic ground vehicle verify the practicality and global convergence of the proposed method, the system exhibits undesired spiral trajectories.

The target capture problem is approached by parameter identification based adaptive motion control designs in [9], [12]. These designs require addition of periodic auxiliary components in agent trajectories for persistence of excitation. Multi-agent target capture and circumnavigation have been studied in a series of works, e.g., [11], [13], [14], where inter-agent and agent-target distance/bearing measurements are utilized for agent coordination and collision avoidance.

Station keeping refers to a variation of the target capture problem where the agent aims at reaching a target location that is implicitly defined by distances to a set of beacons. Real-life applications of station keeping include signal source localization and rescue utilizing sensor networks and multi-agent formation merging, at each step of which a new robotic/vehicular agent joins a robotic/vehicular formation by moving to a location at certain distances from the existing agents in the formation [15]. A switching-based control design is presented in [10] for station keeping in GPS-denied regions, adapting the target capture control design of [8].

Although the aforementioned works have proposed practical methods for the target capture and station keeping problems, none has focused on the robot path characteristics. For instance, the controllers of [8], [10] exhibit undesired spiral paths, and the localization algorithms in [12], [15] require adding extra sinusoidal signals to the vehicle's angular speed. Motivated by this issue, we address the path optimality in the nonholonomic target capture and station keeping problems.

Observing that, in the previous control designs, the noisy robot-target range rate estimations cause deviations in the robot's path, we design a linear quadratic (LQ) controller that aims at minimizing the robot-target distance, without using the range rate estimations. To enable the implementation of the LQ controller, a Luenberger observer is designed to estimate the system states, including the robot-target bearing, utilizing the distance measurements only. We conduct an

[1]A. F. Mostafa and B. Fidan are with the Department of Mechanical and Mechatronics Engineering, University of Waterloo, Canada. ahmedfahim@ieee.org, fidan@uwaterloo.ca

[2]S. Güler is with the Department of Electrical and Electronics Engineering, Abdullah Gul University, Turkey samet.guler@agu.edu.tr

observability analysis which shows that the bearing angle is indeed observable under some feasible conditions. The LQ control design is later extended for the station keeping objective by redefining the states as the distance error variables between the robot and the stationary beacons. Simulations are presented, demonstrating that the proposed controllers outperform the previous designs in terms of path optimality.

II. System and Problem Formulation

We consider the target capture problem studied in [10], aiming to provide an alternative control design that is optimal in terms of the length and smoothness of the generated agent trajectory. Similarly to [10], we focus on driving a constant speed (or a piecewise constant speed) mobile agent to a certain pre-defined neighborhood ball around the target. The problem is formally defined as follows:

Problem 1: Let A denote a single mobile robotic agent moving on 2D plane with location $p_A(t) := [x_A(t),\ y_A(t)]^T \in \Re^2$, which the mobile agent cannot measure due to lack of GPS, and a target T with unknown location $p_T := [x_T,\ y_T]^T \in \Re^2$. Assume that the distance $d(t) := \|p_A(t) - p_T\|$ between A and T can be measured at any given time t while the distance change rate $\dot{d}(t)$ is not available for measurement. Consider the kinematic model

$$\dot{p}_A(t) = v(t) \begin{bmatrix} \cos\theta_A(t) & \sin\theta_A(t) \end{bmatrix}^T, \quad (1)$$

$$\dot{\theta}_A(t) = \omega(t), \quad (2)$$

for the motion of the agent A, where $\theta_A \in (-\pi, \pi]$ denotes the global heading angle from the global x-axis, as illustrated in Fig. 1. Assume that the constant linear speed $v(t) = \bar{v}$ is precisely set as known, and the angular velocity $\omega(t)$ can be accurately applied as control input, with the constraint $-\bar{\omega} \le \omega(t) \le \bar{\omega}$, where $\bar{\omega}$ is the maximum angular velocity bound, at any time t. The control task is to produce $\omega(t)$ so that the mobile agent A converges to the ϵ_d–neighborhood $\mathcal{B}_{\epsilon_d}(p_T) := \{p_A \in \Re^2 \mid \|p_A - p_T\| \le \epsilon_d\}$ of the target T, where ϵ_d is a pre-defined small threshold constant, in finite time, for any given initial location $p_A(0) = p_0$ of A. ■

The kinematic model (1), (2) applies to various mobile agents in the form of ground nonholonomic autonomous vehicles or UAVs hovering at fixed altitude. The linear speed of these platforms can be set at certain constant level depending on the application such that the linear speed controller works as an on/off piecewise function,

$$v(t) = \begin{cases} 0, & d(t) \le \epsilon_d \\ \bar{v}, & otherwise. \end{cases} \quad (3)$$

Note that Problem 1 above is equivalent to Problem 1 of [10] under the control design assertion in Equations (6) and (7) of [10] that sets v and ω to zero once $\mathcal{B}_{\epsilon_d}(p_T)$ is reached.

Defining the (unknown) target bearing angle $\theta_T(t)$ as indicated in Fig. 1, the rate of change of agent-target distance and target bearing angle are derived as follows [6], [10]:

$$\dot{d}(t) = -\bar{v}(t)\cos\theta_T(t), \quad (4)$$

$$\dot{\theta}_T(t) = \omega(t) + \frac{\bar{v}}{d(t)}\sin\theta_T(t). \quad (5)$$

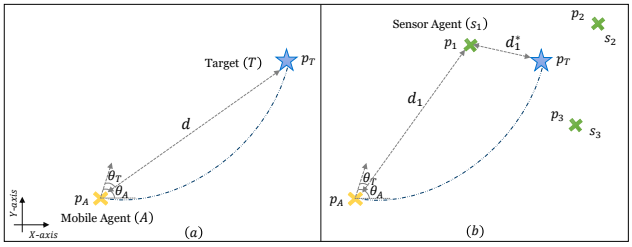

Fig. 1. The problems: (a) Target capturing. (b) Station keeping.

In the previous switching controller designs of [7], [10] to solve Problem 1, the control laws regulate the angular speed $\omega(t)$, depending on the measurements of the agent-target distance $d(t)$ and its change rate $\dot{d}(t)$. These control laws are sensitive to the sensor noises, particularly in measurement of $\dot{d}(t)$, and they do not guarantee optimality for the resultant agent trajectories. These trajectories indeed are observed to contain redundant loop intervals [10].

As different from [7], [10], this paper aims to solve Problem 1 optimally in terms of the length and smoothness of the path of agent A takes to reach $\mathcal{B}_{\epsilon_d}(p_T)$. To achieve this objective, we follow a linear quadratic approach: We represent the system equations (4), (5) in state-space form, defining the state vector $x(t) = [d(t),\ \theta_T(t)]^T$ and the output signal $y(t) = d(t)$, as

$$\dot{x}(t) = \underbrace{\begin{bmatrix} -\bar{v}\cos x_2(t) \\ \frac{\bar{v}\sin x_2(t)}{x_1(t)} \end{bmatrix}}_{f(x(t))} + \underbrace{\begin{bmatrix} 0 \\ 1 \end{bmatrix}}_{B} \omega(t), \quad (6)$$

$$y(t) = \begin{bmatrix} 1 & 0 \end{bmatrix} x(t), \quad (7)$$

and formulate the optimization task as minimization of a quadratic cost function in the form

$$J = \frac{1}{2}\int_0^\infty \left[x^T(t) Q_c x(t) + r_c \omega^2(t)\right]\, dt, \quad (8)$$

where Q_c is a positive definite matrix and r_c is a positive scalar, respectively, defining the cost weights of state regulation error and the control signal magnitude. Note that the control signal magnitude is related to the smoothness of the agent path through (1) and (2). Therefore, the mobile agent determines the shortest smooth path to the target location by optimally solving the objective function in (8).

In the next two sections, we design an LQ optimal control scheme for generating the control signal ω such that (8) is minimized. The design will also involve a state estimation scheme that is composed of a Luenberger state observer for an equivalent state-space representation and state mapping with this equivalent representation, for estimating the unknown state variable θ_T from the available output measurement y. The overall system block diagram of the proposed state estimation and control scheme is given in Fig. 2.

III. Linear Quadratic Control Design

The base state-feedback LQ control law for solving Problem 1 and minimizing (8) is derived by first fictitiously

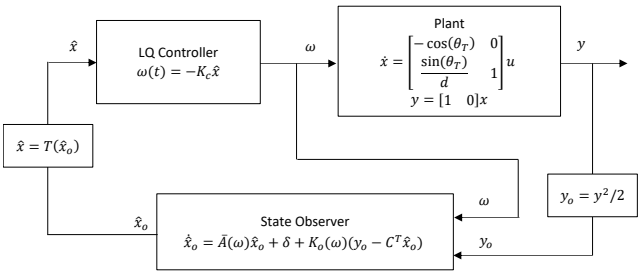

Fig. 2. Overall system block diagram

assuming that the state x is known and following the design steps in [16], [17] as

$$\omega(t) = -K_c(t)x(t), \tag{9}$$
$$K_c(t) = r_c^{-1}B^T(x(t))P_c(t), \tag{10}$$

where $P_c = P_c^T > 0$ is obtained solving the Riccati equation

$$\dot{P}_c = P_cA^T + AP_c - P_cBr_c^{-1}B^TP_c + Q_c = 0. \tag{11}$$

In the actual LQ control law, the unknown state x will be replaced with its estimate $\hat{x}$, which will be generated using a state observer to be designed in Section IV, as follows:

$$\omega(t) = -K_c(t)\hat{x}(t), \tag{12}$$
$$K_c(t) = r_c^{-1}B^T(\hat{x}(t))P_c(t), \tag{13}$$

where $P_c = P_c^T > 0$ is the solution of the Riccati equation

$$\dot{P}_c = P_cA^T(\hat{x}) + A(\hat{x})P_c - P_cBr_c^{-1}B^TP_c + Q_c = 0. \tag{14}$$

To facilitate the LQ control design, the system equation (6) is linearized around the instantaneous state estimation point $\hat{x}(t)$ as follows:

$$\dot{x} = f(x) + B\omega \cong f(\hat{x}) + A(x - \hat{x}) + B\omega, \tag{15}$$
$$= Ax + B\omega + f(\hat{x}) - A\hat{x}, \tag{16}$$

where

$$A = \left.\frac{\partial f}{\partial x}\right|_{\hat{x}} = \begin{bmatrix} 0 & \bar{v}\sin\hat{x}_2 \\ \frac{-\bar{v}\sin\hat{x}_2}{\hat{x}_1^2} & \frac{\bar{v}\cos\hat{x}_2}{\hat{x}_1} \end{bmatrix}, \ \hat{x}_1 \neq 0, \tag{17}$$

and $f(\hat{x}) - A\hat{x}$ is treated as a known disturbance term.

IV. State Observer Design

The state estimate vector $\hat{x}(t)$ can be produced following different approaches. One approach is Luenberger observer design based on the following equivalent rewrite of the state equation (6), (7) by defining the state vector $x_o = [d^2/2, \ d\sin\theta_T, \ d\cos\theta_T]^T$ and the output signal $y_o = d^2/2$. Deriving

$$\dot{x}_{o1} = d\dot{d} = -x_{o3}v, \tag{18}$$
$$\dot{x}_{o2} = \dot{d}\sin\theta_T + d\cos\theta_T\dot{\theta}_T \tag{19}$$
$$= -v\cos\theta_T\sin\theta_T + d\cos\theta_T\omega + v\cos\theta_T\sin\theta_T$$
$$= x_{o3}\omega$$
$$\dot{x}_{o3} = \dot{d}\cos\theta_T - d\sin\theta_T\dot{\theta}_T \tag{20}$$
$$= -v\cos^2\theta_T - d\sin\theta_T\omega - v\sin^2\theta_T$$
$$= -v - x_{o2}\omega,$$

we obtain

$$\dot{x}_o = \underbrace{\begin{bmatrix} 0 & 0 & -\bar{v} \\ 0 & 0 & \omega \\ 0 & -\omega & 0 \end{bmatrix}}_{\bar{A}(\omega)} x_o + \underbrace{\begin{bmatrix} 0 \\ 0 \\ -\bar{v} \end{bmatrix}}_{\delta} = f(x_o, \ \omega), \tag{21}$$

$$y_o = x_{o1} = \underbrace{\begin{bmatrix} 1 & 0 & 0 \end{bmatrix}}_{C^T} x_o, \tag{22}$$

The Luenberger observer is designed following the design steps in [16], [17] as

$$\dot{\hat{x}}_o = \bar{A}(\omega)\hat{x}_o + \delta + K_o(\omega)(y_o - C^T\hat{x}_o), \tag{23}$$

where the observer gain $K_o(\omega) = [K_{o1}(\omega), \ K_{o2}(\omega), \ K_{o3}(\omega)]^T$ is calculated instantaneously such that

$$\bar{A}(\omega) - K_o(\omega)C^T = \begin{bmatrix} -K_{o1}(\omega) & 0 & -\bar{v} \\ -K_{o2}(\omega) & 0 & \omega \\ -K_{o3}(\omega) & -\omega & 0 \end{bmatrix} \tag{24}$$

is stable with eigenvalues having some preset values.

For example to have all the three eigenvalues at $-\lambda$ for a given positive number $\lambda > 0$, the characteristic polynomial of (24) needs to be

$$\det(sI - (\bar{A} - K_oC^T)) = s^3 + 3\lambda s^2 + 3\lambda^2 s + \lambda^3.$$

Hence the corresponding observer gain values are obtained as

$$K_o(\omega) = \begin{bmatrix} K_{o1}(\omega) \\ K_{o2}(\omega) \\ K_{o3}(\omega) \end{bmatrix} = \begin{bmatrix} 3\lambda \\ \frac{\lambda^3 - 3\lambda\omega^2}{\bar{v}\omega} \\ \frac{\omega^2 - 3\lambda^2}{\bar{v}} \end{bmatrix}. \tag{25}$$

The estimate $\hat{x}_o(t)$ is then mapped to $\hat{x}_2(t)$ as

$$\hat{x}_2(t) = \hat{\theta}_T(t) = \angle[\hat{x}_{o3}(t), \ \hat{x}_{o2}(t)]^T, \tag{26}$$

i.e., the angle (from x-axis) of the vector $[\hat{x}_{o3}(t), \ \hat{x}_{o2}(t)]^T$. $\hat{x}_1$ is simply set to measurement of x_1, i.e., $\hat{x}_1(t) = d(t)$.

Another possible approach for generating $\hat{x}_o(t)$ above is Kalman-Bucy filter (KBF) design based on the following slightly modified model of the state dynamics, introducing the process noise ν_x and the output measurement noise ν_y:

$$\dot{x}_o(t) = \bar{A}(\omega(t))x(t) + \delta + \nu_x(t), \tag{27}$$
$$y(t) = x_{o1}(t) + \nu_y(t). \tag{28}$$

The KBF is designed as

$$\dot{\hat{x}}_o = \bar{A}(\omega)\hat{x}_o + \delta + K_o(y_o - C^T\hat{x}_o), \tag{29}$$

where the observer gain is calculated by

$$K_o(t) = P_o(t)Cr_o^{-1}, \tag{30}$$

r_o is the constant noise covariance matrix of ν_y, $P_o(t)$ is obtained by solving the Riccati equation

$$P_o\bar{A}^T + \bar{A}P_o - P_oCr_o^{-1}C^TP_o + Q_o = 0, \tag{31}$$

Q_o is the noise measurement covariance matrix of ν_x. The alternative approach based on KBF is planned to be studied in detail in a future work.

V. Observability and Stability Analysis

To ensure the existence of a state estimator for the design presented in Section III, observability of the system (21), (22) needs to be studied. For observability analysis, we use the *observability matrix* O of the system (21), (22), which is defined in terms of the Lie derivatives $L_f^0 y_o = y_o$, $L_f^1 y_o = \frac{\partial y_o}{\partial x} f$,..., $L_f^i y_o = \frac{\partial L^{i-1}}{\partial x_o} f$,... as

$$O = \begin{bmatrix} \frac{\partial L_f^0 y_o}{\partial x_{o1}} & \frac{\partial L_f^1 y_o}{\partial x_{o1}} & \cdots & \frac{\partial L_f^i y_o}{\partial x_{o1}} & \cdots \\ \frac{\partial L_f^0 y_o}{\partial x_{o2}} & \frac{\partial L_f^1 y_o}{\partial x_{o2}} & \cdots & \frac{\partial L_f^i y_o}{\partial x_{o2}} & \cdots \\ \frac{\partial L_f^0 y_o}{\partial x_{o3}} & \frac{\partial L_f^1 y_o}{\partial x_{o3}} & \cdots & \frac{\partial L_f^i y_o}{\partial x_{o3}} & \cdots \end{bmatrix}^\top. \quad (32)$$

Observing that

$$\begin{aligned} L_f^0 y_o &= x_{o1} = d^2/2, \\ L_f^1 y_o &= -\bar{v} x_{o3}, \\ L_f^2 y_o &= \bar{v}\omega x_{o2} + 2\bar{v}^2, \\ L_f^3 y_o &= \bar{v}\omega x_{o3}, \\ L_f^4 y_o &= -\bar{v}\omega^2 x_{o2} - \bar{v}^2\omega, \ldots \end{aligned}$$

One can write (32) explicitly as

$$O = \begin{bmatrix} 1 & 0 & 0 \\ 0 & 0 & -\bar{v} \\ 0 & \bar{v}\omega & 0 \\ 0 & 0 & \bar{v}\omega \\ 0 & -\bar{v}\omega^2 & 0 \\ \vdots & \vdots & \vdots \end{bmatrix}. \quad (33)$$

Next, we state the observability properties of the system (6), (7).

Proposition 1: The mobile agent's kinematic system model (21), (22) is locally weakly observable if for any time interval $t \in [t_0,\ t_1],\ t_1 > t_0$, it holds that $\omega(t) \neq 0$.

Proof: The model (21), (22) is locally weakly observable if its observability matrix O is full-rank [18]. Hence, the result directly follows from (33). ∎

Locally weakly observability implies that the system states can be estimated by observing the input and output signals over a finite time interval $t_0 \leq t \leq t_1$. Notably, the other rows of O do not alter the observability condition stated in Proposition 1. Thus, the control law can be designed so as to satisfy the observability condition.

The following theorem states the stability and convergence properties of the closed-loop system.

Theorem 1: Consider the plant (6), (7), the LQ controller (12)-(14), and the Luenberger state observer (23), (25). Assume that the initial state estimates and control input satisfy $\hat{x}_{o1}(0) = d^2(0)/2,\ \hat{x}_{o2}^2(0) + \hat{x}_{o3}^2(0) = d^2(0),\ \omega(0) \neq 0$, and the Riccati equation (14) always has a solution. Then, it is guaranteed that $p_A(t)$ asymptotically converges to $\mathcal{B}_{\epsilon_d}(p_T)$.

Proof: As long as $p_A(t)$ is outside the disc $\mathcal{B}_{\epsilon_d}(p_T)$, $v(t) = \bar{v}$, and the LQ controller (12)–(14), and the Luenberger state observer (23), (25) are well defined. Further, the gain assignment (25) and the observer (23) guarantee that the estimation error $\tilde{x}_o = \hat{x}_o - x_o$ has stable dynamics

$$\dot{\tilde{x}}_o = (\bar{A} - K_o C^T)\tilde{x}_o, \quad (34)$$

and converges to zero exponentially, i.e. $\hat{x}_o(t)$ converges to $x_o(t)$ exponentially. Therefore, $\hat{x}$ converges to $x(t)$ exponentially, and hence the actual control law (12) converges to the ideal LQR law (9) exponentially and x asymptotically converges to zero [16], [17], which further implies that $p_A(t)$ asymptotically converges to $\mathcal{B}_{\epsilon_d}(p_T)$. ∎

VI. Station Keeping

In this section, we extend the LQ control and state observer designs of Sections III and IV for path-optimal solution of the station keeping problem in GPS-denied environments studied in [7], [10], which is formally defined as follows.

Problem 2: Consider a set $S := \{s_1, ..., s_N\}$ of $N \geq 3$ beacon sensor nodes with (non-collinear) 2D locations $p_i \in \Re^2,\ \forall s_i \in S$, a target T located at p_T with distance $d_i^* := \|p_T - p_i\|$ to each $s_i \in S$, and a mobile robotic agent A with position $p_A(t)$ at time t and kinematics (1), (2). The beacon locations p_i and the target location p_T are unknown to the agent A. Denote the distance between each beacon s_i and the agent A by $d_i(t) := \|p_A(t) - p_i\|$. Assuming that the constant linear speed $v(t) = \bar{v}$ is set as known, the control goal is to generate the angular velocity $\omega(t)$ to steer A to p_T, guaranteeing asymptotic convergence of $p_A(t)$ to $\mathcal{B}_\epsilon(p_T) := \{p_A \in \Re^2 \mid \|p_A - p_T\| \leq \epsilon\}$, where $\epsilon > 0$ is a pre-defined small threshold constant, as $t \to \infty$ for any $p_A(0)$. ∎

The rate of change of the distance between A and each $s_i \in S$ is derived as follows [10]

$$\dot{d}_i(t) = -\bar{v}\cos\theta_i(t), \quad (35)$$

$$\dot{\theta}_i(t) = \omega(t) + \frac{\bar{v}}{d_i(t)}\sin\theta_i(t), \quad (36)$$

where $\theta_i \in [0, 2\pi)$ is A's heading angle with respect to s_i.

For our LQ optimal control design for addressing Problem 2, we define a new system state vector

$$x_s = \left[x_{s_1}^T, \cdots, x_{s_N}^T\right]^T \in \Re^{2N},\ \ x_{s_i} = [d_i,\ \theta_i]^T, \quad (37)$$

and rewrite (35), (36) in state-space form as

$$\dot{x}_{s_i}(t) = \underbrace{\begin{bmatrix} -\bar{v}\cos x_{s_{i2}}(t) \\ \frac{\bar{v}\sin x_{s_{i2}}(t)}{x_{s_{i1}}(t)} \end{bmatrix}}_{f(x_{s_i})} + \underbrace{\begin{bmatrix} 0 \\ 1 \end{bmatrix}}_{B}\omega(t), \quad (38)$$

$$y_i = \begin{bmatrix} 1 & 0 \end{bmatrix} x_{s_i}(t),\ \ \forall i \in \{1, ..., N\}. \quad (39)$$

When considering each beacon sensor s_i, the overall state space model in (38) can be reduced to the case of the target capture problem in (6). Hence, the state estimation scheme (23), (25), (26) can be utilized for estimating the heading angle $\theta_i(t)$. However, for convenience of addressing Problem 2, we formulate the corresponding LQ optimal control problem with respect to the distance error terms

$$e_i(t) = d_i^* - d_i(t) = d_i^* - \begin{bmatrix} 1 & 0 \end{bmatrix} x_{s_i},\ \ \forall i \in \{1, ..., N\}. \quad (40)$$

To augment these error terms to (38), (39), we define the error integral state w such that $\dot{w} = [e_1, ..., e_N]^T$, leading to the augmented state space model (for $i \in \{1, ..., N\}$)

$$\dot{x}_{a_i}(t) = A_{a_i} x_{a_i}(t) + B_a \omega(t) + \begin{bmatrix} 0 \\ 0 \\ 1 \end{bmatrix} d_i^*, \quad (41)$$

$$y_{a_i}(t) = \begin{bmatrix} 1 & 0 & 0 \end{bmatrix} x_{a_i}(t), \quad (42)$$

$$x_{a_i}(t) = \begin{bmatrix} x_{s_i}(t) & w_i(t) \end{bmatrix}, \quad (43)$$

$$A_{a_i} = \begin{bmatrix} A_i & & 0 \\ -\begin{bmatrix} 1 & 0 \end{bmatrix} & & 0 \end{bmatrix}, \quad B_a = \begin{bmatrix} 0 \\ 1 \\ 0 \end{bmatrix}, \quad (44)$$

where A_i are the system matrices, as derived in (17). To generalize the augmented state space model in (41) and (42), let $i_e(t) = \arg \max_{i \in \{1,...,N\}} |e_i(t)|$. The quadratic cost for Problem 2 is defined as

$$J = \frac{1}{2} \int_0^\infty [e_{i_e}^T(t) Q_{cs} e_{i_e}(t) + r_{cs} \omega^2(t)] \, dt, \quad (45)$$

where the penalty parameters Q_{cs} and r_{cs} are chosen in such a way that gives the highest priority to the distance error terms (40). Hence, the LQ control law to address Problem 2 is obtained as

$$\omega(t) = -K_{cs}(t) \hat{x}_{a_{i_e}}(t), \quad (46)$$

$$K_{cs}(t) = r_{cs}^{-1} B_a^T P_{cs}(t), \quad (47)$$

where $\hat{x}_{a_{i_e}}$ is estimate of state $x_{a_{i_e}}$ obtained via the corresponding Luenberger observer, and $P_{cs} = P_{cs}^T > 0$ is obtained by solving the Riccati equation

$$\dot{P}_{cs} = P_{cs} A_{a_{i_e}}^T + A_{a_{i_e}} P_{cs} - P_{cs} B_a r_{cs}^{-1} B_a^T P_{cs} + Q_{cs} = 0. \quad (48)$$

A feasible solution is guaranteed under the conditions of Proposition 1.

VII. Simulation Results

This section presents the results of our simulation tests for the target capture and station keeping control schemes designed in Sections III, IV, and VI. In the target capture simulation tests, the noisy robot agent-target distance measurements are produced by adding zero-mean white Gaussian noise $\eta \sim \mathcal{N}(0, \sigma^2)$ on the actual distance d, where the standard deviation $\sigma = 0.07$ m of η is chosen based on the characteristics of some commercially available TOF-based ultra-wide-band sensors. To illustrate the advantages of the LQ target capture control scheme of Sections III and IV, we compare the results with the control scheme of [10] for the same simulation setting. The simulation parameters of the control schemes are set as follows: $Q_c = diag\{0.5, \ 1\}$, $r_c = 100$ for target capture (Prob. 1), $Q_{cs} = diag\{0, \ 0, \ 0.1\}$, $r_{cs} = 100$ for station keeping (Prob. 2). Initial heading angle is $\theta_A(0) = \frac{\pi}{2}$ rad for Prob. 1, and $\theta_A(0) = \frac{\pi}{3}$ rad for Prob. 2. The maximum linear velocity is $\bar{v} = 0.5$ m/s. Inter-distance tolerance is set as $\epsilon = 0.5$ m for Prob. 1 and $\epsilon = 0.3$ m for Prob. 2. The switching controller parameters for [10] are $c = \alpha = 1, \ \lambda = 0.1$.

Figures 3–5 show the results of an example simulation setting, among many others tested, where the initial robot location and the target location were set as $p_A(0) = [-2, \ 0.5]^T$ m and $p_T = [3.5, \ 5]^T$ m. In this example simulation setting, the initial robot heading was set as $\theta_A(0) = \pi/2$ rad in the global frame, which corresponds to $\theta_T(0) = 0.68$ rad. The agent paths produced using the proposed controller and those with the controller of [10] are presented in Figures 3–5. It is observed that the LQ control scheme of Sections III,IV produces shorter and smoother agent paths than the control scheme of [10]. For the example with results shown in Figures 4–5, the robot reaches the target location at $t = 13$ seconds with the proposed approach, while it takes $t = 28$ seconds with the controller of [10], and the resultant agent path contains loops which are caused mainly by the range rate measurement/derivation noises.

The station keeping control scheme of Section VI has also been tested via a number of simulations. Here we present one example simulation with the initial robot agent location and the target location set as $p_A(0) = [-4, \ -1]^T$ m and $p_T = [0, \ 0]^T$ m, respectively. The initial agent heading was set as $\theta_A(0) = \pi/3$ rad in the global frame, resulting in a nonzero $\theta_T(0)$. We placed three beacons at random locations nearby the target location. To ensure a feasible solution for the optimization objective in (45), the control parameter r_c is selected in such a way to limit the linear and angular velocities rapid updates. Fig. 6 shows the robot's paths with the proposed controller (46) and the switching-based controller of [10]. Similarly to the target capture scenario, we observe that the proposed controller outperforms the controller of [10] in terms of path length and smoothness.

VIII. Conclusion

In this paper, we studied the problem of capturing and tracking an unknown target location via mobile agents in settings where global positioning is not available, focusing on optimization of the length and smoothness of the agent path towards the target. The problem is solved designing

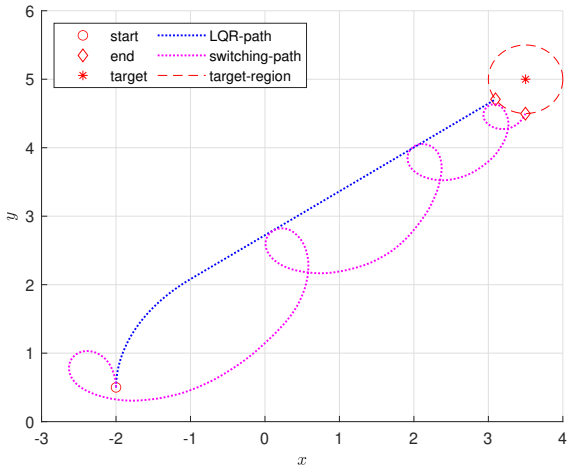

Fig. 3. Mobile agent trajectories for the sample target capture simulation.

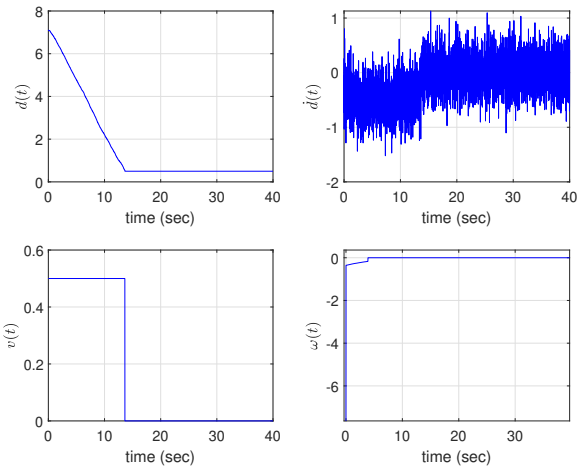

Fig. 4. $d(t)$, $\dot{d}(t)$, $v(t)$, $\omega(t)$ for the sample target capture simulation with the LQR control scheme of Section III.

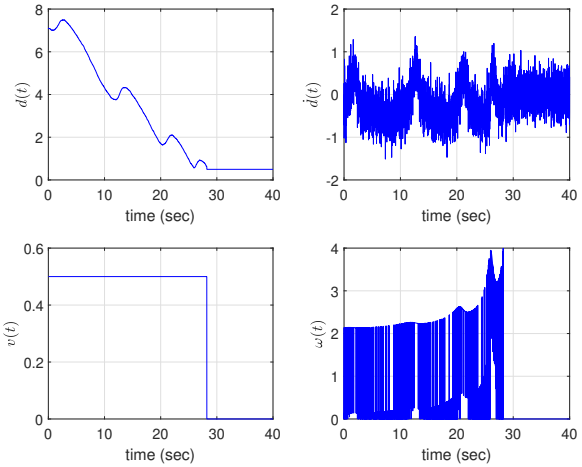

Fig. 5. $d(t)$, $\dot{d}(t)$, $v(t)$, $\omega(t)$ for the sample target capture simulation with the switching controller of [10].

an state-feedback LQ optimal control scheme together with a Luenberger observer based state estimator. The results of different simulation scenarios indicate that the proposed LQ optimal control design produces shorther and smoother agent paths compared to the existing switching-based control designs. The approach is successfully applied to the station keeping problem, i.e., steering the agent to a location that is pre-defined with respect to a set of beacons, as well, where similar favorable characteristics are observed.

ACKNOWLEDGMENTS

This work is supported by the Canadian NSERC Discovery Grant 116806.

REFERENCES

[1] S. M. LaValle, *Planning Algorithms*. Cambridge U. Press, 2006.

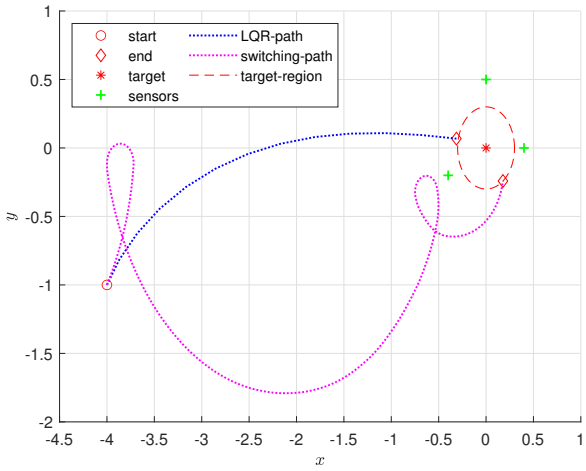

Fig. 6. Mobile agent trajectories for the sample station keeping simulation.

[2] Y. Chen, D. Chang, and C. Zhang, "Autonomous tracking using a swarm of UAVs: A constrained multi-agent reinforcement learning approach," *IEEE Tr. Vehicular Technology*, vol. 69, no. 11, pp. 13 702–13 717, 2020.
[3] X. Wang, L. T. Yang, D. Meng, M. Dong, K. Ota, and H. Wang, "Multi-UAV cooperative localization for marine targets based on weighted subspace fitting in SAGIN environment," *IEEE Internet of Things J.*, vol. 9, no. 8, pp. 5708–5718, 2021.
[4] J. Cochran and M. Krstic, "Nonholonomic source seeking with tuning of angular velocity," *IEEE Tr. Automatic Control*, vol. 54, no. 4, pp. 717–731, 2009.
[5] A. Hashemi, Y. Cao, D. Casbeer, and G. Yin, "UAV circumnavigation of an unknown target without location information using noisy range-based measurements," in *Proc. American Control Conference*, 2014, pp. 4587–4592.
[6] Y. Cao, "UAV circumnavigating an unknown target using range measurement and estimated range rate," in *Proc. American Control Conference*, 2014, pp. 4581–4586.
[7] Y. Cao, "UAV circumnavigating an unknown target under a GPS-denied environment with range-only measurements," *Automatica*, vol. 55, pp. 150–158, May 2015.
[8] S. Guler and B. Fidan, "Range based target capture and station keeping of nonholonomic vehicles without GPS," in *Proc. European Control Conference*, 2015, pp. 2970–2975.
[9] B. Fidan, A. Camlica, and S. Guler, "Least-squares-based adaptive target localization by mobile distance measurement sensors," *Int. J. of Adapt. Contr. Signal Process.*, vol. 29, no. 2, pp. 259–271, 2015.
[10] S. Guler and B. Fidan, "Target capture and station keeping of fixed speed vehicles without self-location information," *European Journal of Control*, vol. 43, pp. 1–11, 2018.
[11] T.-H. Kim and T. Sugie, "Cooperative control for target-capturing task based on a cyclic pursuit strategy," *Automatica*, vol. 43, no. 8, pp. 1426–1431, 2007.
[12] B. Fidan, S. Dasgupta, and B. D. Anderson, "Adaptive range-measurement-based target pursuit," *Int. J. of Adapt. Contr. Signal Process.*, vol. 27, no. 1-2, pp. 66–81, 2013.
[13] R. Zheng, Y. Liu, and D. Sun, "Enclosing a target by nonholonomic mobile robots with bearing-only measurements," *Automatica*, vol. 53, pp. 400–407, March 2015.
[14] X. Yu and L. Liu, "Cooperative control for moving-target circular formation of nonholonomic vehicles," *IEEE Tr. Automatic Control*, vol. 62, no. 7, pp. 3448–3454, July 2017.
[15] S. Guler, B. Fidan, S. Dasgupta, B. Anderson, and I. Shames, "Adaptive source localization based station keeping of autonomous vehicles," *IEEE Tr. Automatic Control*, vol. 62, no. 7, pp. 3122–3135, July 2017.
[16] F. Lewis, D. Vrabie, and V. Syrmos, *Optimal Control*. Wiley, 2012.
[17] P. Ioannou and B. Fidan, *Adaptive Control Tutorial*. SIAM, 2006.
[18] R. Hermann and A. Krener, "Nonlinear controllability and observability," *IEEE Tr. Automatic Control*, vol. 22, no. 5, pp. 728–740, 1977.